

Quark core impact on hybrid star cooling

Rodrigo Negreiros*

FIAS, Goethe University, Ruth Moufang Str. 1 60438 Frankfurt am Main, Germany

V.A. Dexheimer†

Gettysburg College, Gettysburg, USA

S. Schramm‡

CSC, FIAS, ITP, Johann Wolfgang Goethe University, Frankfurt am Main, Germany

(Dated: March 13, 2012)

In this paper we investigate the thermal evolution of hybrid stars, objects composed of a quark matter core, enveloped by ordinary hadronic matter. Our purpose is to investigate how important are the microscopic properties of the quark core to the thermal evolution of the star. In order to do that we use a simple MIT bag model for the quark core, and a relativistic mean field model for the hadronic envelope. By choosing different values for the microscopic parameters (bag constant, strange quark mass, strong coupling constant) we obtain hybrid stars with different quark core properties. We also consider the possibility of color superconductivity in the quark core. With this simple approach, we have found a set of microscopic parameters that lead to a good agreement with observed cooling neutron stars. Our results can be used to obtain clues regarding the properties of the quark core in hybrid stars, and can be used to refine more sophisticated models for the equation of state of quark matter.

PACS numbers:

I. INTRODUCTION

Scientists have been trying to determine the equation of state and composition of compact stars for a long time ([1, 2] and references therein). Many of these studies determine constraints for the equation of state of stellar matter so that the predicted stellar properties agree with the observed masses and radii of pulsars. One of the biggest practical shortcomings of such techniques is the lack of accurate and reliable observations for the radii of compact stars, which makes constraining the equation of state very challenging. A recent paper [3] has put forth unprecedented constraints on the mass-radius diagrams of pulsars, which would certainly make the range of possible equations of state narrower. The analysis of this data however has been questioned [4], and therefore is not universally accepted. Another method that might be used to complement the results provided by the analysis of the structure of the compact star is the examination of the thermal evolution of the object. The cooling of a compact star is intrinsically connected to its microscopic composition, and therefore different microscopic models might lead to different thermal evolutions. The results of the theoretical investigations might then be compared with the wealth of observed data of the thermal properties of compact stars [5, 6]. In this paper we will follow the thermal evolution approach, and with this probe the

composition of compact stars.

In the following we will consider the thermal evolution of hybrid stars (HS), which are objects composed of a strange quark matter core, enveloped by ordinary hadronic matter [1, 2]. In this work, neutron stars (NS) denote objects made up solely of hadronic matter.

The cooling of neutron stars is dominated by neutrino emission for the first 1000 years (possibly more for the slow cooling scenario) [7], being replaced by surface photon emission after that. Amongst the neutrino emission mechanisms, the direct Urca (DU hereafter) process sets itself apart by being one of the most efficient ones, with emissivity of the order of 10^{26} erg cm⁻³ s⁻¹ [8]. Due to momentum conservation, the DU process can only take place if the proton fraction is above a certain value. The actual proton-fraction, above which the DU process is allowed to take place, depends on the underlying microscopic model, and it usually lies between 11%–15%. If a neutron star allows the DU process to take place, the star will exhibit a fast cooling (sometimes also referred to as enhanced cooling). If neutron superfluidity [10, 11] (superconductivity in the case of protons) occurs, pairing will suppress the emission of neutrinos from hadronic processes and smooth the so-called enhanced cooling. The situation for hybrid stars is significantly different, since the presence of deconfined quark matter plays an important role for the cooling of the object. The cooling of hybrid stars has been addressed by many authors [9, 13, 14]. In this work, differently than in references [9, 13, 14], where the cooling of hybrid stars with the same equation of state was studied, we will examine the cooling of hybrid stars with different EoS's for the quark phase. As a result, we will obtain quark cores with different proper-

*Electronic address: negreiros@fias.uni-frankfurt.de

†Electronic address: vantoche@gettysburg.edu

‡Electronic address: schramm@th.physik.uni-frankfurt.de

ties (mass, radius, composition). This should provide us with a measure of how important such properties are for the thermal evolution of hybrid stars, which might aid us in constraining the EoS of compact stars. In order to perform such study we will use a MIT bag model equation of state for the quark phase, and a relativistic-mean-field model EoS for the hadronic phase. The different EoS's for the quark phase are obtained by varying the microscopic parameters of quark matter, namely the bag constant B , the strong interaction constant α_s , and the strange quark mass m_s . The macroscopic structure of the star is obtained by solving the Tolman-Oppenheimer-Volkoff equations [17, 18]. We note that there are more sophisticated models for hybrid stars, see for example [19–21]. However, the relatively simple MIT bag model is appropriate for our study. Due to its phenomenological nature, it permits one to change its microscopic properties with ease, allowing us to obtain quark cores with different properties. This in turn allows us to investigate how such quark cores effectively influence the thermal evolution of hybrid stars. The aim of this procedure is to obtain constraints on the properties of cold quark matter, which then can be used in more sophisticated microscopic calculations.

This paper has the following structure: in Sec. II we describe the microscopic model used, and present the results for the macroscopic structure of the stars; in Sec. III our results for the thermal evolution of the stars discussed in Sec. II are presented; in Sec. IV the role of superconductivity in the quark core is discussed, and the results for the cooling of superconducting hybrid stars are presented; our final remarks and conclusions can be found in Sec. V

II. MODEL

We use a standard relativistic mean field model [1, 2] to describe the hadronic phase, in which the interactions between the baryons are mediated by meson fields ($\sigma, \omega, \bar{\rho}$). The parametrization used is G300, which can successfully reproduce the properties of saturated nuclear matter [22]. We have also allowed pairing in the hadronic phase. The pairing patterns included are the neutron singlet (1S_0) and triplet (3P_2) states, as described in [10, 11]. It is also possible that protons can form pairs, becoming a singlet superconductor; however, the pairing of protons in the core is still not very well understood (see [12] and references therein). For this reason we have decided to take a conservative approach and only consider neutron superfluidity.

For the quark matter description we use the MIT Bag Model, with first order corrections in the strong interaction coupling constant (α_s) [23–26]. In the framework of the MIT Bag Model, the quarks present at the relevant densities are the up, down and strange quarks. It is important to note that, since we are considering massive strange quarks, electrons are required for charge neutrality to be achieved. At lower densities, the electron popu-

TABLE I: Different parameter sets used to obtain the quark matter EoS.

Parameter Set	$B^{1/4}$ (MeV)	m_s (MeV)	α_s
A	139	200	0.7
B	150	175	0.4
C	160	150	0.1

lation is more significant, due to suppression of the massive strange quarks. This is an important phenomenon, that may lead to the formation of ultra-strong electric fields near the surface of bare strange stars [27–30].

In this work we also take into account the possibility of color superconductivity. The pattern that will be considered is the Color-Flavor-Locked phase [31], where all quarks are paired. The CFL phase is the most likely condensation pattern at densities $> 2\rho_0$ [32]. For intermediate densities ($\sim 2\rho_0$) model calculations seem to indicate that quark matter is in a 2SC phase [32]. Another possibility is that quark matter forms a crystalline superconductor, where the momenta of the quark pairs do not add to zero [33, 34]. Since we are considering quark matter only at the inner core of compact stars, we will consider only the CFL phase. It should be noted that one expects corrections to the quark matter EoS if pairing is considered. As shown in [35], such corrections are $\sim \Delta^2 \mu^2$. The authors in ref. [36] have shown, however, that the effects of such corrections to the structure of the star are only noticeable for $\Delta \gtrsim 50$ MeV. Therefore, for the values of Δ considered in this study (0.1 – 10 MeV) they can be safely disregarded. Note that as the small values for the gap (Δ) do not have any appreciable effect on the equation of state, our analysis is still valid for any quark pairing scheme (not necessarily color superconductivity), as long as it affects all quark flavors in similar way. In addition to the quark matter and hadronic matter equation of state, we have also included a crustal EoS, which is given by the Baym-Pethick-Sutherland EoS [37].

The equation of state for the compact star is calculated assuming local charge neutrality and beta equilibrium, as is usual for any bulk system. The phase transition to quark matter is also calculated in the usual way, by connecting the two EoS's at the point where the quark EoS has a higher pressure. The different values used for the quark EoS parameters are illustrated in Table I. These parameters were chosen to cover a wide range of quark core properties (mass, radius and composition), which might potentially lead to different thermal evolution. The final EoS's obtained are shown in Fig. 1, where we plot the pressure as a function of energy density for the different EoS's investigated.

The mass-radius diagram for each EoS studied can be found in Fig. 2. The onset of quark matter can be easily identified as the sharp kink found in the sequences. Note that for simplicity, we adopt a Maxwell construction for the phase transition. We do not expect any qualitative

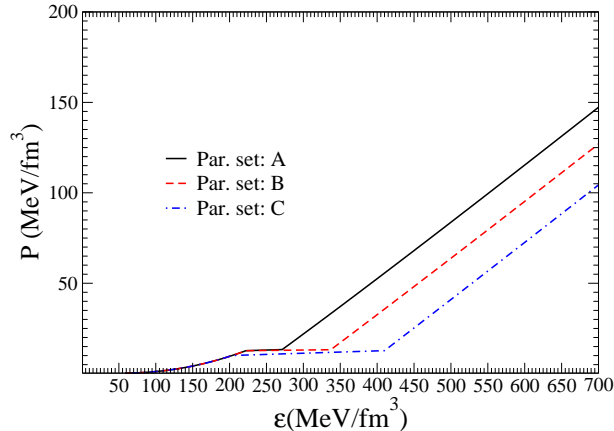


FIG. 1: (Color online) Equation of state for the hadronic and quark phases shown for different parameter sets.

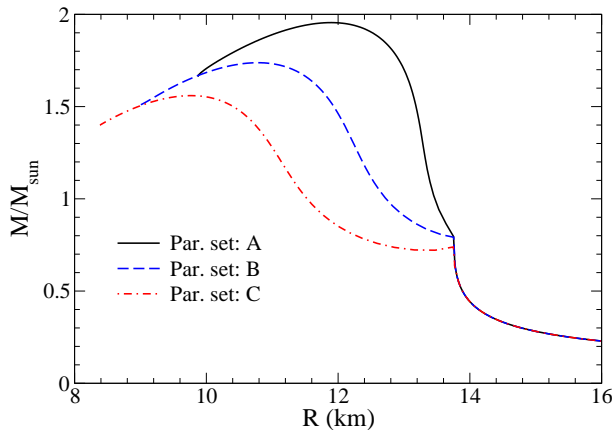


FIG. 2: (Color online) Mass-radius diagram for stars whose equations of state are shown in Fig. 1. The sharp kinks denote the phase transition to quark matter.

change of our conclusions if a more elaborate construction were used.

Given that each of the sequences shown in Fig. 2 has a different quark matter EoS, the quark core of the stars in each sequence should exhibit different properties. This is displayed in Fig. 3 where the mass-radius diagram for the inner quark core of the hybrid stars is shown.

Fig. 3 clearly shows the distinct properties of the quark core for the different EoS's used. We now turn our attention to the thermal evolution of the stars shown in Figs. 2 and 3, and determine the role that the different microscopic compositions play in the thermal evolution of the object.

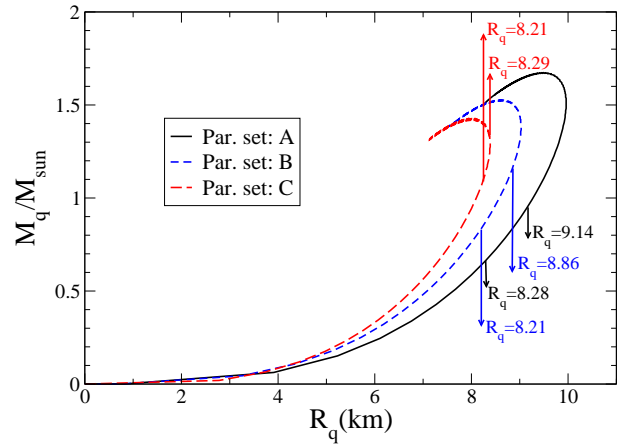


FIG. 3: (Color online) Mass-radius diagram for the quark core of the hybrid stars shown in Fig. 2. Also shown the quark core radius for the stars used in the cooling simulations (see table II)

III. RESULTS

The cooling of compact stars is given by the thermal balance and thermal energy transport equation ($G = c = 1$) [1]

$$\frac{\partial(l e^{2\phi})}{\partial m} = -\frac{1}{\rho \sqrt{1-2m/r}} \left(\epsilon_\nu e^{2\phi} + c_\nu \frac{\partial(T e^\phi)}{\partial t} \right), \quad (1)$$

$$\frac{\partial(T e^\phi)}{\partial m} = -\frac{(l e^\phi)}{16\pi^2 r^4 \kappa \rho \sqrt{1-2m/r}}. \quad (2)$$

In Eqs. 1 and 2, the structure of the star is given by the variables r , $\rho(r)$ and $m(r)$, that represent the radial distance, the energy density, and the stellar mass, respectively. The thermal variables are given by the temperature $T(r, t)$, luminosity $l(r, t)$, neutrino emissivity $\epsilon_\nu(r, T)$, thermal conductivity $\kappa(r, T)$ and specific heat $c_\nu(r, T)$. The boundary conditions of (1) and (2) are determined by the luminosity at the stellar center and at the surface. The luminosity vanishes at the stellar center since at this point the heat flux is zero by definition. At the surface, the luminosity is defined by the relationship between the mantle temperature and the temperature outside of the star [7, 9, 38, 39]. The microscopic inputs that enter Eqs. (1) and (2) are the neutrino emissivities, specific heat and thermal conductivity. For the hadronic phase, the neutrino emission processes considered in this work are the direct Urca, modified Urca and bremsstrahlung processes. A detailed review of the emissivities of such processes can be found in reference [40]. We note that the neutrino emission involving neutrons, and the neutron specific heat are exponentially suppressed as the temperature drops below the neutron superfluidity critical temperature. A description of the

TABLE II: Stellar properties of the stars used for the thermal evolution investigation. All symbols have their usual meaning, and M_q and R_q denotes the mass and radius of the quark matter core, respectively.

Parameter set	M_q/M	R_q (km)	R (km)	M (M_\odot)
A	0.48	8.28	13.26	1.33
	0.60	9.14	13.15	1.55
B	0.62	8.21	12.20	1.33
	0.74	8.86	11.82	1.55
C	0.82	8.21	10.89	1.33
	0.89	8.29	10.03	1.55

paring model, and critical temperature can be found in reference [11]. As for the quark core, we consider the equivalent processes involving quarks. These are the quark direct Urca (QDU), quark modified Urca (QMU), and quark bremsstrahlung processes (QBM). The emissivities of such processes were calculated in [41]. The specific heat of the hadrons in the hadronic phase is given by the usual specific heat of fermions, as described in [5]. For the quark phase we use the specific heat as calculated in [41]. Finally for the thermal conductivity of the hadronic matter, we follow the calculations of [42], and for the quark matter we use the results of [43].

In order to investigate how the difference in the quark cores manifests itself in the thermal evolution, we investigate the cooling of hybrid stars of same mass, but different quark cores. The properties of such stars are listed in Table II.

The thermal evolution of the objects from table II is illustrated in Figs. 4 and 5, which shows the redshifted temperature as a function of the age of the star. We have also plotted prominent observed temperatures for a few pulsars. The data is separated into two sets. The first set, labeled spin-down, contains the temperature of objects whose age are estimated based on their spin-down age. The second set, labeled kinematic, consists of age estimates based on the observed motion of the object with respect to its progenitor supernova remnant. A detailed discussion about the observed data can be found in references [5, 6].

The results indicate that although there is little difference between the cooling of stars with different gravitational masses, we can see a significant difference between stars with different quark core properties. The different cooling tracks exhibited by stars of different models (A, B and C) can be attributed to the differences in the quark core. Figs. 4 and 5 show that for a more massive quark core, the cooling of the star becomes faster. This is a result of the microscopic composition of such models, that allow for more intense presence of the QDU (due to a higher electron population). It is also important to understand that regardless of the total mass of the star, the hadronic layer plays the same role. This is indicated by the similar cooling behavior shown for the purely hadronic stars of masses 1.33 and 1.55 M_\odot

shown Figs. 4 and 5. The reason for such behavior is the presence of the hadronic superfluidity, which suppresses the hadronic DU process. Without superfluidity a neutron star with higher mass could exhibit a faster cooling than a lower mass star, since the DU process could be active in the former but not in the latter. The fact that the hadronic layer plays the same role, regardless of the total mass of the object, is very important for our analysis, since it allows us to better understand the effects introduced by the different quark cores in the thermal evolution of the star

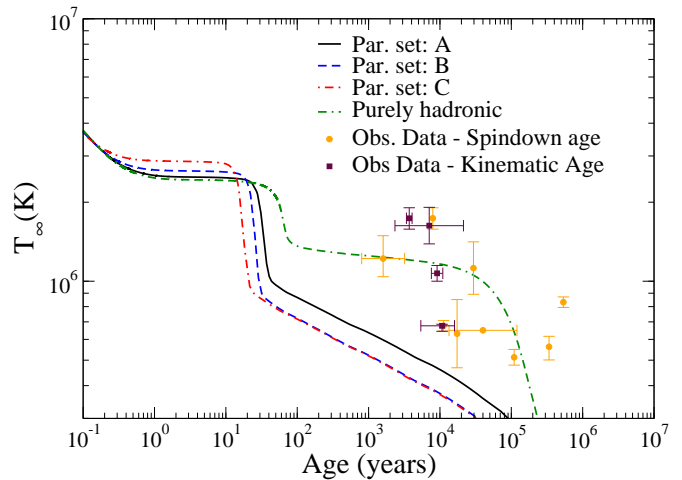


FIG. 4: (Color online) Cooling of hybrid stars with gravitational mass of 1.33 M_\odot . T_∞ denotes the temperature observed at infinity, and the x-axis the age in years. Also plotted is the cooling of the equivalent purely hadronic star with the same mass. Two sets of observed data were used, one whose age estimate is based on spin-down rate, and another that is based on the kinematic age [5, 6].

IV. ROLE OF COLOR SUPERCONDUCTIVITY

It seems clear that the presence of the quark core enhances the cooling of the star to a point that is in clear disagreement with the observed data, whereas the purely hadronic model seems to do a (slightly) better job. We note however that results presented so far do not represent the whole picture. As mentioned in section II, strange quark matter is expected to be in a superconducting phase. The most likely condensation pattern for high densities is the Color-Flavor-Locked phase, in which all quarks are paired. Because of pairing the direct Urca process is suppressed by a factor $e^{-\Delta/T}$, and the modified Urca and the Bremsstrahlung process by a factor $e^{-2\Delta/T}$, for $T \leq T_c$, where Δ is the gap parameter for the CFL phase and T_c is the critical temperature below which strange matter undergoes a phase transition into CFL matter. In addition to changes in the neutrino emissivities, the specific heat of quark

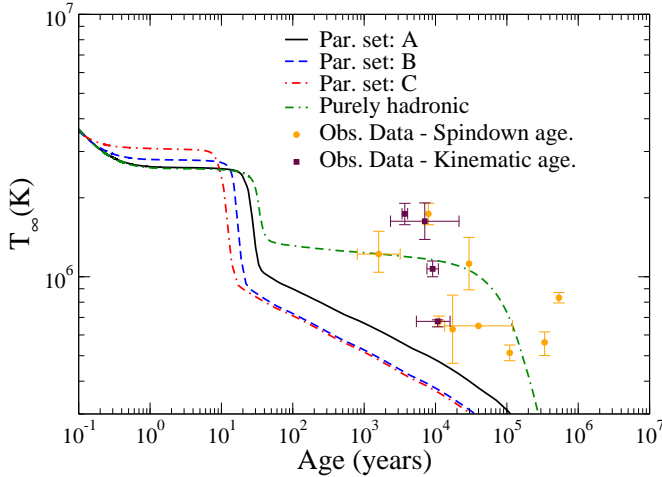


FIG. 5: (Color online) Same as Figure 4, but for stellar mass of $1.55 M_{\odot}$.

matter is also modified, being reduced by the factor $3.2(T_c/T) * (2.5 - 1.7(T/T_c) + 3.6(T/T_c)^2)e^{-\Delta/T}$ [9]. The critical temperature for the CFL phase is currently not known, although it is believed to be smaller than the standard Bardeen-Cooper-Schrieffer ($T_c \simeq 0.57\Delta$), due to instanton–anti-instanton effects. In this work we follow the footsteps of the authors in [9], and use $T_c = 0.4\Delta$.

In addition to the traditional neutrino emissivities, one could also include the emissivities from massive and massless Goldstone modes. These emissions, as discussed in [15], are small, and should have small effects on the thermal evolution of the object if more powerful emission processes are present. In addition to that, we have also not considered the contributions of photons, and Goldstone modes to the thermal conductivity of CFL quark matter [16]. If these modes are considered, the thermal conductivity of quark matter should be higher than that calculated in [43]. Not denying that such contributions are important, we do not expect that they would strongly affect our results. As discussed in [16], a higher thermal conductivity would only mean that the quark core will be in thermal equilibrium with the hadronic phase more quickly. We intend to include these contributions in future calculations.

We now show in Figs. 6 and 7 the results for the cooling of hybrid stars of $1.55 M_{\odot}$, whose quark core is composed of strange quark matter in the CFL phase with $\Delta = 0.1$ MeV and $\Delta = 1.0$ MeV, respectively.

As discussed in the last section, the hadronic layer plays a small role in the cooling of hybrid stars, with the quark core dominating the thermal evolution (at least for the first 1000 years). Following this logic it is only obvious that the introduction of the CFL phase should alter the cooling substantially. This is indeed the case, as shown in Figs. 6 and 7. We see that objects with $\Delta = 0.1$

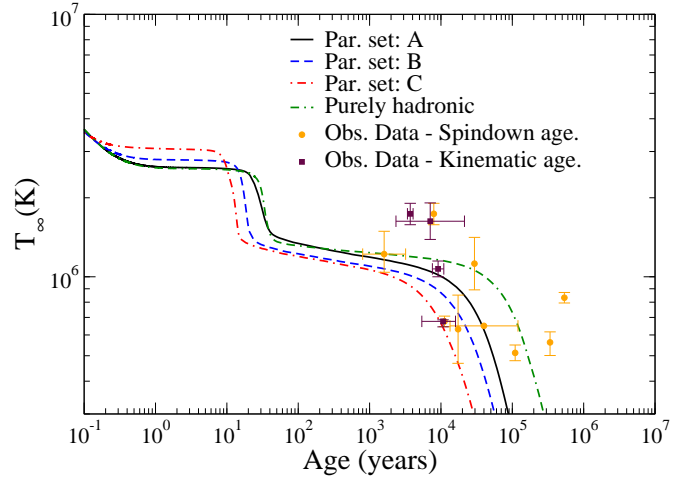


FIG. 6: (Color online) Cooling of hybrid stars with gravitational mass of $1.55 M_{\odot}$, and $\Delta = 0.1$ MeV. Axis and observed data are the same as in Fig. 4

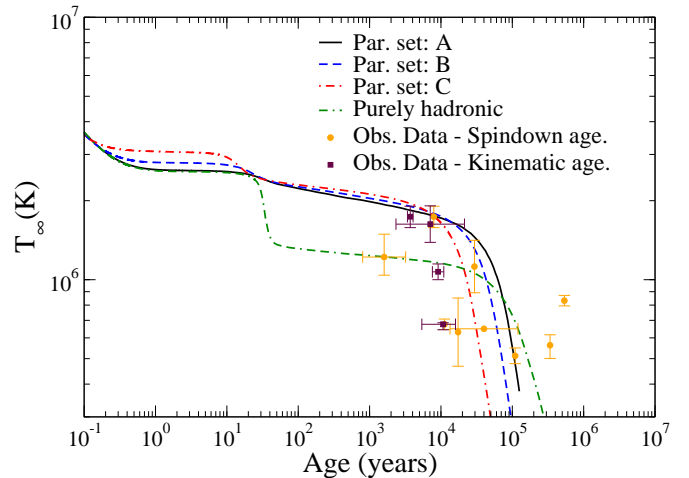


FIG. 7: (Color online) Same as Fig. 7 but for $\Delta = 1.0$ MeV.

MeV exhibit a much slower cooling than their unpaired counterparts (Figs. 4 and 5). The slower cooling is due the suppression of the neutrino emission processes in the quark core resulting from quark pairing. Fig. 7 shows that a higher value of Δ will result in even slower cooling as a higher Δ will lead to stronger suppression. We note, however, that for $\Delta \geq 1.0$ the resulting thermal evolution is almost the same as that of $\Delta = 1.0$. This is due to the fact that the exponential $\exp(-\Delta/T)$ effectively saturates for $\Delta > 1.0$ MeV.

Figs. 6 and 7 also show that hybrid stars, whose quark cores are in a CFL phase, agree relatively well with the

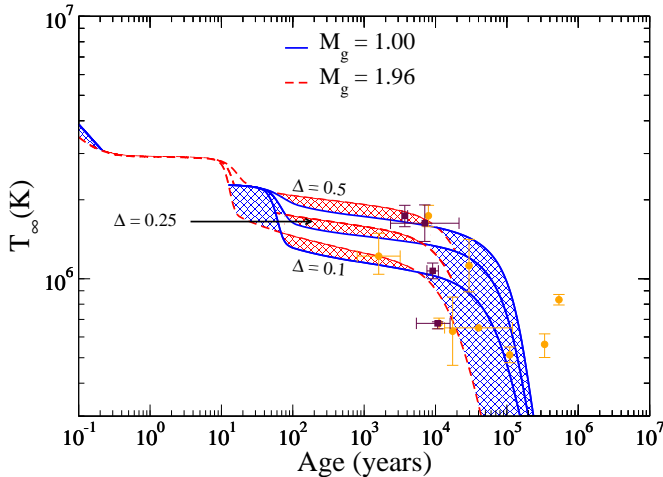


FIG. 8: (Color online) Cooling of hybrid stars (model A), for different values of the CFL gap (Δ).

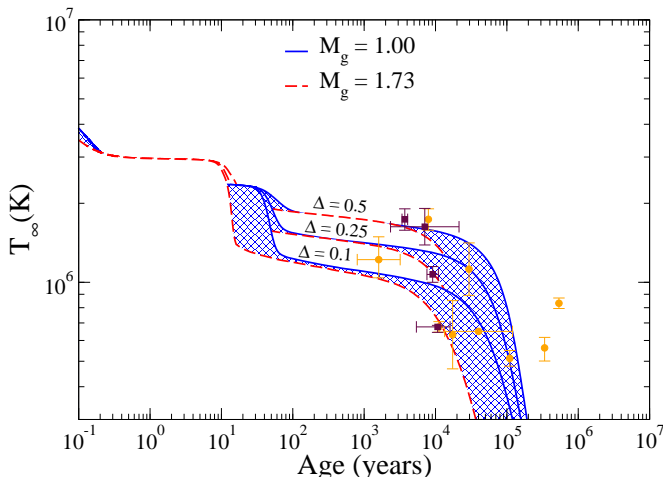


FIG. 9: (Color online) Cooling of hybrid stars (model B), for different values of the CFL gap (Δ).

observed data. We see, however, that smaller values of Δ (~ 0.1 MeV) lead to agreement with only a few objects (those with lower temperatures), while $\Delta \sim 1.0$ MeV leads to agreement with those with higher temperature. This behavior hints that the best agreement will possibly be obtained for intermediate values of Δ , if one means to interpret the whole set of observed data as hybrid stars. In order to investigate this we explore different values of Δ , and calculate the cooling band spanned by the cooling curves of stars with $1.00 M_\odot$ and the maximum mass of each respective parameter set. This result is shown in Figs. 8-10.

The results shown in Figs. 8-10 indicate that the ob-

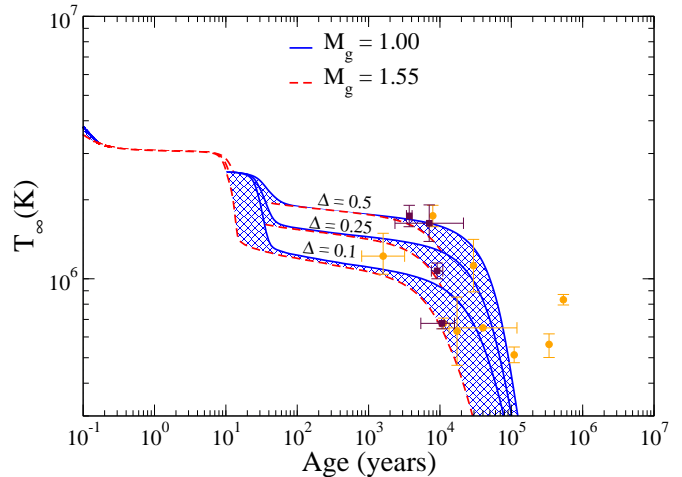


FIG. 10: (Color online) Cooling of hybrid stars (model C), for different values of the CFL gap (Δ).

served data can be better explained by hybrid stars whose quark phase is in a CFL state with pairing gaps between 0.25 and 0.5 MeV. These results also show us that the difference between models B and C is very subtle, with both these models describing the same data points. Model A, however, is substantially different, as can be seen in Fig. 8. One can see that as opposed to B and C, in the range of age between 10^2 to 10^4 years, the most massive star in Model A exhibits a slower cooling. This behaviour is due to less massive quark cores in this model. We note that there are still two objects that do not fall within the range of the cooling curves, these are the two oldest stars in the graph. We believe that this might be due to uncertainties in the estimate of their spin-down age. As pointed out in [44], the spin-down age may be an over-estimation of their actual age. If indeed that is the case these objects may be younger than they appear, in which case they may fall into the range defined by the cooling curves. The analysis of the age estimate of these objects, however, is beyond the scope of this paper.

V. DISCUSSION & CONCLUSIONS

It is the purpose of this paper to investigate the importance of the quark core properties to the cooling of hybrid stars. Although there have been a handful of papers analyzing different models for hybrid stars, and their agreement with observational mass and radius constraints [13, 14, 20, 21, 45, 46], we intend to provide a complementary study, in which observed temperatures of pulsars, together with cooling simulations of hybrid stars are used to infer the importance of the microscopic properties of the quark core to the thermal evolution. To achieve that goal, we have used a MIT bag model to

describe the quark phase, and a relativistic mean field model for the hadron phase. Different values for microscopic parameters of the quark phase were used, which led to quark cores with different properties.

The results obtained indicate that it is possible to explain the observed thermal properties of pulsars with a hybrid star model. Furthermore, the best agreement with the observed data was obtained for hybrid stars with a CFL quark core with $\alpha_s = 0.4$, $B^{1/4} = 150$ MeV, $m_s = 175$ MeV and with $\Delta = 0.25 - 1.0$ MeV. We note that parameter set A ($\alpha_s = 0.7$, $B^{1/4} = 139$ MeV, $m_s = 200$) was also in good agreement with the observed data. Furthermore, this parameter set has the advantage of agreeing with the observed mass of J1614-2230 ($1.96 \pm 0.04 M_\odot$) [47]. Parameter set A assumes, however, that $\alpha_s = 0.7$ which might be considered too high for the first order corrections used in the calculation of the quark matter EoS. Because of this, the results obtained from parameter set A should be regarded with care, which is the reason why we selected parameter set B (which also exhibits satisfactory agreement with cooling data, albeit not with the mass of J1614-2230) as that with the best agreement with the observed cooling data (given its more reliable microscopic model). We can however, learn something from the results of parameter set A, i.e. that the cooling will present a better agreement with the observed data for models that yield less massive quark cores, and lower electron population (as in parameter set A). For higher values of the gap parameter ($\Delta \geq 10$ MeV), the band of possible cooling curves becomes too narrow, which worsens the agreement with the observed data. We note that this result is independent of the equation of state used for the hadronic matter, as long as the latter presents a suppression of fast neutrino emission processes. This is very reasonable, considering that the hadronic layer is constrained to the lower density regime, in which neutron superfluidity is very likely to take place.

It is important to remember that in this paper we have considered a somewhat simple microscopic model, and a more sophisticated study, considering for example different degrees of freedom, and chiral symmetry restoration [20, 21, 46] would certainly be of interest. Work in that direction is currently in progress. We believe, however, that even for a more sophisticated microscopic model our conclusions should still hold. If so, this would imply that a quark core with the properties similar to those of the best case scenario (see parameters above) should provide the best agreement with the observed data.

We note that, although we have considered neutron superfluidity, we have not included proton superconduc-

tivity in the core, nor the emission of neutrinos due to the pair breaking/formation process. The aforementioned processes were the subject of recent papers [48, 49] aimed at modeling the observed temperature evolution of the neutron star in Cas A. The inclusion of proton superconductivity is still speculative, and since we do not have a clear picture of how (or if) it manifests itself in a high-density environment (see ref. [12] and references therein), we chose to take a conservative approach and only consider neutron superfluidity. One could also include the pair breaking/formation process, however, this should have little effect on our results. Differently from references [48, 49], we allow fast neutrino processes to take place (hence the dip in the cooling curve at around 100 years), which (even suppressed by pairing) dominate over the other neutrino emission processes. Therefore, by allowing fast emission processes in the core, we cannot describe the observed behaviour of the neutron star in Cas A. We note that the cooling of high mass stars of parameter set A (in a CFL phase) present temperatures and ages comparable to those of Cas A, but the slope of the temperature evolution is wrong. This indicates that either the neutron star in Cas A has a mass smaller than the direct Urca threshold (and thus has no fast neutrino emission processes), or that our model needs further refinements. We should also point out that the authors of [50] have shown that a hybrid star model can be used to model the observed behavior of Cas A, indicating that the recent observations do not rule out hybrid stars. Furthermore, it has been recently proposed that the behavior of Cas A can be explained as the late onset of the Direct Urca process in spinning down neutron stars [51]. We note that the same principle could be applied to hybrid stars, where the transition to quark matter could be delayed due to spin-down. This study will be the object of a future investigation.

The purpose of this paper was to determine if quark cores with different properties would lead to different thermal evolution, in a way that one could use this information to constrain the microscopic properties of quark matter in hybrid stars. We have found a set of parameters that leads to a reasonably good agreement with the observed data of cooling neutron stars, although not all of them agree with the observed mass of J1614-2230. It is evident that there is room for improvement in the approach we used to model quark matter microscopically, and it is our intent to use the results and constraints put forth in this work, in addition to the latest observational data, to refine the current models for the EoS of quark matter.

[1] F. Weber, *Pulsars as astrophysical laboratories for nuclear and particle physics*, 1st ed. (Institute of Physics, Bristol, 1999)

[2] N. K. Glendenning, *Compact stars : nuclear physics, particle physics, and general relativity*, 1st ed. (Springer, 2000)

- [3] F. Ozel, G. Baym, and T. Guver, arXiv/1002.3153(2010)
- [4] A. W. Steiner, J. Lattimer, and E. F. Brown, arXiv/1005.0811(2010)
- [5] D. Page, J. Lattimer, M. Prakash, and A. W. Steiner, The Astrophysical Journal Supplement Series **155**, 623 (2004)
- [6] D. Page, J. Lattimer, M. Prakash, and A. W. Steiner, The Astrophysical Journal **707**, 1131 (2009)
- [7] D. Page, U. Geppert, and F. Weber, Nuclear Physics A **777**, 497 (2006)
- [8] J. Lattimer, C. Pethick, M. Prakash, and P. Haensel, Physical review letters **66**, 27012704 (1991)
- [9] D. Blaschke, T. Klahn, and D. Voskresensky, The Astrophysical Journal **533**, 406412 (2000)
- [10] C. Schaab, F. Weber, M. Weigel, & N. K. Glendenning, Nuclear Phys A **605**, 531 (1996).
- [11] K. P. Levenfish, & D. G. Yakovlev, Astronomy Letters **20**, 43 (1994).
- [12] D. Page, M. Prakash, J. M. Lattimer, & A. W. Steiner, astro-ph/1110.5116 (2011).
- [13] H. Grigorian, D. Blaschke, and D. Voskresensky, Physical Review C **71**, 1 (2005)
- [14] D. Blaschke, D. Voskresensky, and H. Grigorian, Nuclear Physics A **774**, 815 (2006)
- [15] P. Jaikumar, M. Prakash, and T. Schäfer, Physical Review D **66**, 1 (2002)
- [16] I. Shovkovy and P. Ellis, Physical Review C **66**, 1 (2002)
- [17] R. Tolman, Physical Review **55**, 364 (1939)
- [18] J. Oppenheimer and G. Volkoff, Physical Review **55**, 374 (1939)
- [19] H. Grigorian, D. Blaschke, and D. Aguilera, Physical Review C **69**, 1 (2004)
- [20] R. Negreiros, V. Dexheimer, and S. Schramm, Physical Review C **82**, 1 (2010)
- [21] V. A. Dexheimer and S. Schramm, Physical Review C **81** (2010)
- [22] N. K. Glendenning, Nuclear Physics A **493**, 521 (1989)
- [23] A. Chodos, R. Jaffe, K. Johnson, C. Thorn, and V. Weisskopf, Physical Review D **9**, 3471 (1974)
- [24] A. Chodos, R. Jaffe, K. Johnson, and C. Thorn, Physical Review D **10**, 2599 (1974)
- [25] E. Farhi and R. Jaffe, Physical Review D **30**, 2379 (1984)
- [26] F. Weber, Progress in Particle and Nuclear Physics **54**, 193 (2005)
- [27] C. Alcock, E. Farhi, and A. Olinto, The Astrophysical Journal **310**, 261 (1986)
- [28] V. Usov, Physical Review D **70**, 14 (2004)
- [29] R. Negreiros, F. Weber, M. Malheiro, and V. Usov, Physical Review D **80**, 083006 (2009)
- [30] R. P. Negreiros, I. Mishustin, S. Schramm, & F. Weber, Physical Review D **82**, 103010 (2010).
- [31] M. Alford, Annual Review of Nuclear and Particle Science **51**, 131 (2001)
- [32] M. Alford, A. Schmitt, K. Rajagopal, and T. Schäfer, Reviews of Modern Physics **80**, 1455 (2008)
- [33] M. Alford, J. Bowers, and K. Rajagopal, Physical Review D **63**, 074016 (2001)
- [34] J. Bowers and K. Rajagopal, Physical Review D **66**, 065002 (2002)
- [35] G. Lugones and J. E. Horvath, Physical Review D **66**, 1 (2002)
- [36] M. Alford and S. Reddy, Physical Review D **67**, 1 (2003)
- [37] G. Baym, C. Pethick, and P. Sutherland, The Astrophysical Journal **170**, 299 (1971)
- [38] E. H. Gudmundsson, C. J. Pethick, and R. I. Epstein, The Astrophysical Journal **259**, L19 (1982)
- [39] R. I. E. E. H. Gudmundsson, C. J. Pethick, The Astrophysical Journal **272**, 286 (1983)
- [40] D. Yakovlev, A. D. Kaminker, O. Y. Gnedin, and P. Haensel, Physics Reports **354**, 1 (2001)
- [41] N. Iwamoto, Annals of Physics **141**, 1 (1982)
- [42] E. Flowers and N. Itoh, The Astrophysical Journal **250**, 750 (1981)
- [43] P. Haensel, Nuclear Physics B - Proceedings Supplements **24**, 23 (1991)
- [44] C. M. Espinoza, a. G. Lyne, M. Kramer, R. N. Manchester, & V. M. Kaspi, The Astrophysical Journal **741**, L13 (2011).
- [45] A. Kurkela, P. Romatschke, A. Vuorinen, and B. Wu, arXiv/1006.4062(2010)
- [46] D. Blaschke, J. Berdermann, and R. Lastowiecki, arXiv/1009.1181(2010)
- [47] P. B. Demorest, T. Pennucci, S. M. Ransom, M. S. E. Roberts, & J. W. T. Hessels, Nature **467**, 1081 (2010).
- [48] D. Page, M. Prakash, J. Lattimer, & A. Steiner, Physical Review Letters **106**, 081101 (2011).
- [49] P. S. Shternin, D. G. Yakovlev, C. O. Heinke, W. C. G. Ho, & D. J. Patnaude, Monthly Notices of the Royal Astronomical Society: Letters **412**, L108-L112 (2011).
- [50] T. Noda, M. Hashimoto, Y. Matsuo et al, astro-ph/1109.1080
- [51] R. Negreiros, S. Schreamm, & F. Weber, astro-ph/1103.3870